1521-009X/49/11/1003–1015$35.00
DRUG METABOLISM AND DISPOSITION

https://doi.org/10.1124/dmd.121.000612
Drug Metab Dispos 49:1003–1015, November 2021

Predicting Maternal-Fetal Disposition of Fentanyl Following Intravenous and Epidural Administration Using Physiologically Based Pharmacokinetic Modeling

Sara Shum, Danny D. Shen, and Nina Isoherranen

Department of Pharmaceutics, University of Washington, Seattle, Washington

Received July 14, 2021; accepted August 10, 2021

ABSTRACT

Fentanyl is an opioid analgesic used to treat obstetrical pain in parturient women through epidural or intravenous route, and unfortunately can also be abused by pregnant women. Fentanyl is known to cross the placental barrier, but how the route of administration and time after dosing affects maternal-fetal disposition kinetics at different stages of pregnancy is not well characterized. To address this knowledge gap, we developed a maternal-fetal physiologically based pharmacokinetic (mf-PBPK) model for fentanyl to evaluate the feasibility to predict the maternal and fetal plasma concentration-time profiles of fentanyl after various dosing regimens. As fentanyl is typically given via the epidural route to control labor pain, an epidural dosing site was developed using alfentanil as a reference drug and extrapolated to fentanyl. Fetal hepatic clearance of fentanyl was predicted from CYP3A7-mediated norfentanyl formation in fetal liver microsomes (intrinsic clearance = 0.20 ± 0.05 μl/min/mg protein). The developed mf-PBPK model successfully captured fentanyl maternal and umbilical cord concentrations after epidural dosing and was used to simulate the concentrations after intravenous dosing (in a drug abuse situation). The distribution kinetics of fentanyl were found to have a considerable impact on the time course of maternal:umbilical cord concentration ratio and on interpretation of observed data. The data show that mf-PBPK modeling can be used successfully to predict maternal disposition, transplacental distribution, and fetal exposure to fentanyl.

SIGNIFICANCE STATEMENT

This study establishes the modeling framework for predicting the time course of maternal and fetal exposures of fentanyl opioids from mf-PBPK modeling. The model was validated based on fentanyl exposure data collected during labor and delivery after intravenous or epidural dosing. The results show that mf-PBPK modeling is a useful predictive tool for assessing fetal exposures to fentanyl opioid therapeutic regimens and potentially can be extended to other drugs of abuse.

Introduction

Fentanyl and other opioid analgesics are commonly used together with local anesthetics to relieve pain during surgical procedures. Depending on the procedure, fentanyl is typically given epidurally or intrathecally for regional anesthesia, although similar plasma concentrations are observed after epidural and intravenous infusions (Ellis et al., 1990; Baxter et al., 1994). Fentanyl is also used to treat parturient women during labor and delivery through epidural and intrathecal injections (Grangier et al., 2020). Although undesirable maternal and fetal side effects such as hypotension, nausea, and pruritus in the mom (Loftus et al., 1995; Poole, 2003; Grangier et al., 2020) and bradycardia and lower neurologic and adaptive capacity score in the newborns (Loftus et al., 1995; Van De Velde, 2005) were reported after the use of fentanyl during labor and delivery, these effects are considered transient, and the use of epidural fentanyl appears safe in parturient women (Reynolds et al., 2002; Kesavan et al., 2018). There has been a growing incidence of opioid use disorder in the general population and in pregnant women (Schauberger et al., 2014; Palmsten et al., 2015; Haas et al., 2018), and intravenous fentanyl is currently a drug of abuse in pregnant women (Haight et al., 2018). This parenteral route results in higher peak concentrations (C_{max}) in the mom than what is observed after epidural administration and could pose a higher risk to the fetus. However, little is known about the fetal exposures and time course of fetal fentanyl concentrations in drug abuse situations with intravenous fentanyl.

Fentanyl is a synthetic opioid more potent than morphine (Stanley, 1992). It is a lipophilic (logP = 4.05) weak base (pKa = 8.99)

This work was supported by the National Institutes of Health grant [P01 DA032507], NIH NCATS training grant [TL1 TR002318], and the Elmer M. Plein Endowed Research Fund at the University of Washington.

NI reports consultancy agreements with Boehringer-Ingelheim, Xenon Pharmaceuticals, and Johnson & Johnson; honoraria from the National Institutes of Health and as an Associate Editor with Clinical and Translational Science, and Drug Metabolism and Disposition. All other authors have no conflicts interests.

dx.doi.org/10.1124/dmd.121.000612.

ABBREVIATIONS: AAFE, absolute average fold error; B/P ratio, blood-to-plasma ratio; CL, clearance; CLint, hepatic intrinsic clearance; $CL_{int,u}$, unbound hepatic intrinsic clearance; CLpd,adipose, unbound permeability clearance from the epidural fluid to the epidural adipose tissue; CLpd,vein, unbound permeability clearance from the epidural fluid to the epidural vein; CSF, cerebrospinal fluid; FLM, fetal liver microsomes; f_u, fraction unbound in plasma; HPLC-MS/MS, high performance liquid chromatography with tandem mass spectrometry; IVIVE, in vitro to in vivo extrapolation; Km, concentration of substrate at half of the maximal product formation rate; K_p, tissue partitioning coefficients; logP, partition coefficient; MA, maternal artery; mf-PBPK, maternal-fetal physiologically based pharmacokinetic; MV, maternal vein; Papp, apparent permeability; PBPK, physiologically based pharmacokinetic; PD, pharmacodynamic; PK, pharmacokinetics; pKa, negative logarithm of the acid dissociation constant; Qepidural, blood flow to the epidural space; t_{max}, time to reach C_{max}; UA, umbilical artery; UV, umbilical vein; V, volume; V_{ss}, steady-state volume of distribution.

(Rodgers and Rowland, 2007) that is widely distributed in the body with an estimated steady-state volume of distribution (V_{ss}) of 4 l/kg in healthy adults (McClain and Hug, 1980; Nozari et al., 2019). The elimination of fentanyl is mainly through hepatic metabolism mediated by CYP3A4 with less than 5% of intravenous dose eliminated unchanged in urine (Ziesenitz et al., 2015). The pharmacokinetics (PK) of fentanyl after epidural injections in parturient women has been reported in multiple studies (Desprats et al., 1991, 1995; Moisés et al., 2005; Haidl et al., 2018), and the steady-state concentrations after intravenous and epidural infusion (same rate) of fentanyl to women after cesarean-section were shown to be similar (Ellis et al., 1990). Fentanyl crosses the placenta and has been detected in the umbilical vein (UV) within 30 minutes of an epidural dose to parturient women (Desprats et al., 1991, 1995; Moisés et al., 2005; Haidl et al., 2018). However, the UV to maternal venous (MV) plasma concentration ratios after epidural and intravenous fentanyl dosing have only been reported from single timepoints during labor. Notably, the reported UV/MV concentration ratios vary widely after epidural or IV administration of fentanyl; UV/MV ratios were 0.3–3.4 within an hour after epidural bolus dose (Desprats et al., 1991, 1995; Moisés et al., 2005; De Barros Duarte et al., 2009), 0.3–1.9 within an hour after intravenous dosing (Morley-Forster et al., 2000), and 0.6–3.1 at 1–15 hours after epidural infusion (Bader et al., 1995; Loftus et al., 1995; Haidl et al., 2018). Part of the variability could be attributed to rapid changes in maternal and fetal plasma concentrations during distribution of fentanyl to the fetus. At present, fetal pharmacokinetics of fentanyl after intravenous or epidural dosing is not well characterized or understood sufficiently.

We hypothesized that the maternal-fetal disposition of fentanyl after an epidural or intravenous dosing can be predicted using physiologically based pharmacokinetic (PBPK) modeling. To test this hypothesis a maternal-fetal-PBPK (mf-PBPK) model of fentanyl was developed with incorporation of a novel epidural dosing site. The goal of this study was to predict the fetal concentration-time profile of fentanyl after maternal epidural and intravenous doses to aid in understanding maternal and fetal risks of maternal fentanyl exposure during pregnancy.

Materials and Methods

Development of a Maternal-Fetal Physiologically Based Pharmacokinetic Model with an Epidural Dosing Site. An mf-PBPK model was developed in MATLAB and the Simulink platform (R2019b; MathWorks, Natick, MA). The structure of the model was modified from a previously published mf-PBPK model, which includes a 14-compartment maternal PBPK model and a 7-compartment fetal PBPK model linked together by a placenta compartment (Zhang et al., 2017a). A similar structural model without the placenta and fetal PBPK model was used for simulations of drug disposition in nonpregnant population (Fig. 1). Drug distribution to all organs was modeled as perfusion-limited process as validated in a previously developed PBPK model of fentanyl (Huang and Isoherranen, 2020). The clearances into and out of the placenta incorporated potential permeability-limited kinetics using a method established previously (Zhang and Unadkat, 2017) to simulate maternal-fetal disposition using clearance scaled from Caco-2 permeability. Simulated concentrations were sampled from the same site as reported in the observed studies. To accomplish this, a previously developed peripheral sampling site (arm vein) (Huang and Isoherranen, 2020) was incorporated into the maternal PBPK model. Additionally, to model the maternal-fetal disposition after epidural dosing, an epidural dosing site model was developed and incorporated in parallel to the other organ compartments in the maternal PBPK model.

The structure of the epidural dosing site model was developed based on known physiology of the human epidural space. The epidural space is located between the ligamentum flavum posteriorly and the posterior longitudinal ligament anteriorly surrounding the spinal cord outside of the dura mater, which is filled mainly with adipose tissue (Richardson and Groen, 2005; Becske and Nelson, 2009; Desjardins et al., 2011). The epidural space is highly vascularized and receives oxygenated blood from the spinal arteries superiorly from the aorta and drains to the internal vertebral venous plexus that empties into the inferior vena cava (Richardson and Groen, 2005; Becske and Nelson, 2009). An epidural bolus injection is usually given with volume between 4 and 20 ml, which creates a sheath of solution surrounding the epidural space upon injection (Hogan, 2002). The dose will either partition into the epidural adipose tissue or be taken up by the venous system according to the direct connection between the epidural space and the venous system (Buffington et al., 2011). Based on the physiology, the epidural dosing site was modeled such that the dose is given into the epidural fluid surrounding the epidural space. From there, the dose can either passively diffuse to and partition into the adipose tissue or passively diffuse to and be taken up by the epidural vein (i.e., internal vertebral venous plexus) (Fig. 1). Distribution to CSF (through the dura mater) was not included in the model, as most of the volume injected into the epidural space has been shown to stay outside of the dura mater (Hogan, 2002), and the rate of fentanyl transfer from the epidural space to the CSF has been shown to be significantly slower than that to the epidural adipose tissue and venous plasma (Ummenhofer et al., 2000). A sensitivity analysis was also performed to assess whether a direct connection between the CSF and the vasculature can be kinetically discerned from plasma kinetics.

The physiologic parameters (i.e., organ volumes and blood flows) of the nonpregnant model (including the arm sampling site model) were adopted from a previously published PBPK model (Huang and Isoherranen, 2020). The physiologic parameters of the mf-PBPK model to match a pregnant woman at term (gestational week 40) were calculated using previously published equations to describe physiologic changes of pregnant women and fetuses during gestation (Abduljalil et al., 2012; Zhang et al., 2017b). A CYP3A4 induction factor of 1.99 was used in the maternal-fetal model based on previous observation that CYP3A4 expression increased by 1.99-fold during late pregnancy (Hebert et al., 2008). Parameters without published values in pregnant women were assigned to be the same as those in the nonpregnant women (Table 1). For the drugs studied, the transplacental clearances were assumed to be mediated by passive processes, although active transport could be incorporated in the model if present, and only unbound drug was assumed to passively diffuse across the placenta (i.e., syncytiotrophoblast monolayer).

The physiologic parameters for the epidural dosing site were taken from those for the lumbar vertebrae region (L1 to L5), which is where epidural injection is typically given. The volume of the epidural adipose tissue ($V_{epidural,adipose}$) in the lumbar region has been reported to be around 3.5 ml (Walker et al., 2019), and the blood flow to the epidural space ($Q_{epidural}$) was calculated first based on the reported velocity of blood flow in spinal arteries into the lumbar region and the diameter of spinal arteries (arterial blood flow = 1.12 l/h) (Arslan et al., 2011; Espahbodi et al., 2013). Since the spinal blood drains through the internal vertebral venous plexus (inside the epidural space) and the external vertebral venous plexus (outside of epidural space), the $Q_{epidural}$ was assumed to be 50% of the arterial blood flow (i.e., 0.56 l/h). The volume of the epidural vein ($V_{epidural,vein}$) was assumed to be the same as $V_{epidural,adipose}$ (3.5 ml). The volume of the epidural fluid ($V_{epidural,fluid}$) was assumed to be the same as the typical epidural injection volume of 10 ml. The clearances from the epidural fluid to the epidural adipose tissue and the epidural vein were assumed to be mediated by passive processes, which allow only unbound drug to cross the adipocyte cell membrane and the venous endothelium lining. The bioavailability after epidural administration was assumed to be 100% based on the previous observations that similar steady-state concentration was observed after intravenous and epidural infusions at the same dosing rate (Ellis et al., 1990; Baxter et al., 1994) (Table 1).

Sensitivity Analyses of the Epidural Dosing Site Model. The absorption profile of epidurally dosed drugs including the rate of absorption and the fraction of dose sequestered in the epidural adipose tissue have been shown to depend on the physicochemical properties (i.e., molecular weight, logP, pKa, etc) of the dosed drug (Ummenhofer et al., 2000; Bernards et al., 2003). Hence, sensitivity analyses were performed for the final epidural dosing site model to identify the sensitive physicochemical and physiologic parameters. To do this, a hypothetical drug X model was developed. Drug X was assumed to be a neutral compound with tissue partitioning coefficients (K_p's), blood-to-plasma (B/P) ratio, and plasma fraction unbound (f_u) assumed to be 1 unless the parameter was assessed in the sensitivity analysis. The hepatic clearance of drug X was assumed to be 45 l/h (hepatic extraction ratio = 0.5), and the renal clearance of drug X was

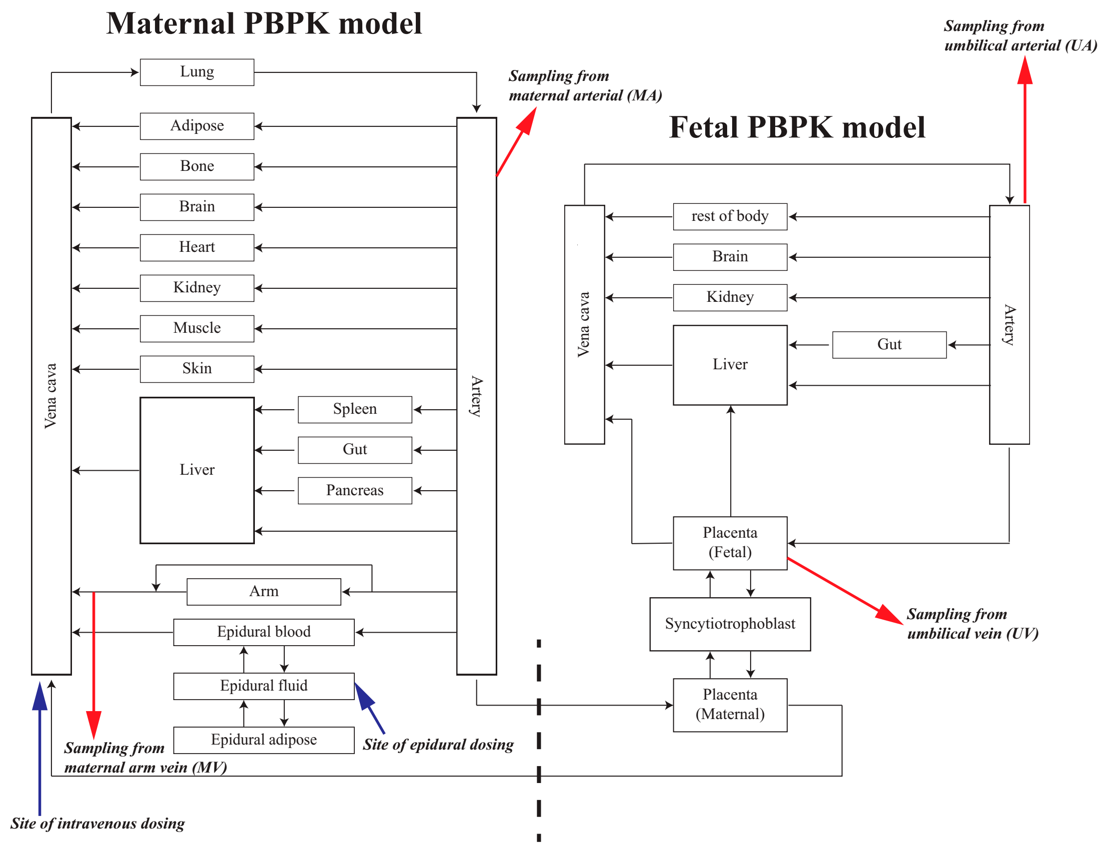

Fig. 1. Model structure of the maternal-fetal PBPK (mf-PBPK) model with an arm sampling site and an epidural dosing site incorporated. The blue arrows indicate the intravenous and epidural dosing sites to the mother, and the red arrows indicate the MA and MV plasma sampling locations for the mother, and the UA and UV plasma sampling sites for the fetus. A nonpregnant PBPK model used in this study was structurally identical as the maternal PBPK model, but the linkage to the placenta and fetal PBPK model was removed as indicated by the dashed line. The arm compartment includes anastomoses in the arm as previously described (Huang and Isoherranen, 2020) indicated by an arrow bypassing the arm compartment.

assumed to equal to the glomerular filtration rate (i.e., 7.2 l/h). The bidirectional unbound permeability clearance from the epidural fluid to the epidural adipose tissue ($CL_{pd,adipose}$) of drug X was calculated to be 0.003 l/h using the estimated surface area of the epidural adipose tissue based on reported anatomic dimensions of the epidural fat in the lumbar region (8.6 cm^2) (Reina et al., 2009) and an assumed permeability (P_{app}) of 100 × 10^{-6} cm/s. Since the exact surface area for the epidural venous compartment is not well characterized, the bidirectional unbound permeability clearance from the epidural fluid to the epidural vein ($CL_{pd,vein}$) of drug X was assumed to be the same as $CL_{pd,adipose}$ (i.e., 0.003 l/h).

Four sets of three-dimensional local sensitivity analyses were performed by varying two parameters at a time to evaluate the impact of covarying parameters on the simulated C_{max} and t_{max} after a single epidural bolus dose of 100 μg of drug X. The C_{max} and t_{max} were chosen as the measurements of the rate of absorption after epidural administration. The range of values explored for each parameter was divided into 25 equal steps, and the possible combinations of the two varying parameters were simulated (i.e., 25 x 25 = 625 simulations per sensitivity analysis). To identify the sensitive physicochemical parameters that affect drug disposition after epidural dose, sensitivity analyses were performed with (1) varying $CL_{pd,adipose}$ and $CL_{pd,vein}$ each from 0.00003 to 0.3 l/h (i.e., P_{app} from 1×10^{-6} to 1×10^{-2} cm/s), (2) varying f_u from 0.1 to 1 (only in the epidural venous plasma to assess the effect of protein binding on the distribution kinetics at the epidural site to ignore the possible concurrent effect on hepatic and renal clearances) and $K_{p,epidural,adipose}$ from 0.01 to 100 (while keeping the K_p of the adipose tissue for the rest of the body constant at 1 to avoid significant changes in whole body V_{ss}). To evaluate the effect of epidural blood flow on drug disposition after epidural dose, sensitivity analysis was performed with (3) $Q_{epidural}$ from 0.056 to 5.6 l/h (10% to 10-fold of the physiologic value of 0.56 l/h) and $CL_{pd,vein}$ from 0.00003 to 0.3 l/h [same range as (1)]. To evaluate whether parallel routing between epidural fluid and the vasculature via the CSF (i.e., epidural fluid → CSF → spinal vein) is kinetically discernible, additional sensitivity analysis was performed with (4) asymmetric $CL_{pd,vein}$, in which the ratio of $CL_{pd,vein}$ from epidural vein to epidural fluid ($CL_{pd,veintofluid}$) to $CL_{pd,vein}$ from epidural fluid to epidural vein ($CL_{pd,fluidtovein}$) varied from 0.1 to 1.

Verification of the Epidural Dosing Site Model Using Alfentanil as a Model Compound. Since the exact surface areas for the epidural vein are not well characterized to afford prediction of $CL_{pd,vein}$ based upon permeability estimates, the $CL_{pd,vein}$ was first optimized and verified using a structurally similar compound, alfentanil, as a model compound. The $CL_{pd,vein}$ for alfentanil was estimated using the observed plasma concentration of alfentanil after epidural administration. Then, the $CL_{pd,vein}$ of fentanyl was scaled using the optimized $CL_{pd,vein}$ of alfentanil and the Caco-2 permeability of alfentanil and fentanyl, using a similar approach as previously described to scale placental passive diffusion clearance (Zhang and Unadkat, 2017). To do this, a PBPK model of alfentanil was developed. The B/P ratio, plasma f_u, and K_p's of alfentanil were collected from literature (Bower and Hull, 1982; Bjorkman et al., 1990; Palm et al., 1999), and the parameter values are listed in Table 2. Alfentanil is exclusively eliminated through hepatic metabolism mediated by CYP3A4 with only 1% of the dose excreted unchanged in urine (Stanski and Hug, 1982). The unbound hepatic intrinsic clearance of alfentanil ($CL_{int,u}$ = 185 l/h) was calculated using the hepatic well stirred model from the averaged total body clearance (average CL = 13.5 l/h) observed after intravenous dose of alfentanil to healthy subjects reported in five studies (Ferrier et al., 1985; Kharasch et al., 1997, 2004, 2011; Phimmasone and Kharasch, 2001). The alfentanil model was validated using the plasma concentrations observed in the above five intravenous dosing studies. Simulations of alfentanil plasma concentration-time profiles after intravenous dose were performed using the nonpregnant PBPK model and the same dose and sampling site (arm vein) as in the original studies. One of the five

TABLE 1

Physiologic parameters of the PBPK models with epidural dosing site (GW = gestational week)

	Nonpregnant Model[a]		Maternal Model[b] (GW 40)		Fetal Model[b] (GW 40)	
	l Volume	*l/h* Blood flow	*l* Volume	*l/h* Blood flow	*l* Volume	*l/h* Blood flow
Adipose	15	16.2	22.6	24.4	–	–
Bone	10	13.1	10	13.1	–	–
Brain	1.4	35.6	1.4	35.6	0.375	13.28
Gut	1.2	46.8	1.2	46.8	0.1	3.95
Heart	0.33	12.5	0.33	12.5	–	–
Kidney	0.31	60	0.31	64.7	0.031	4.16
Liver	1.8	90	1.8	90	0.129	16.42
Lung	0.53	308	0.53	391	–	–
Pancreas	0.098	3.1	0.098	3.1	–	–
Skin	2.6	18.1	2.6	18.1	–	–
Muscle	28	57.3	28.17	57.3		
Spleen	0.18	6.2	0.18	6.2	–	–
Blood	5	–	5.64	–	0.42	–
Rest of body	–	–	–	–	2.384	47.41
Arm adipose	0.0338	0.0709	0.0338	0.0709	–	–
Arm muscle	0.268	0.29	0.268	0.29	–	–
Arm skin	0.0363	0.218	0.0363	0.218	–	–
Arm anastomoses	–	0.06432	–	0.06432	–	–
Epidural adipose	0.0035	–	0.0035	–	–	–
Epidural fluid	0.01	–	0.01	–	–	–
Epidural vein	0.0035	0.56	0.0035	0.56	–	–
Placenta	–	–	0.659	49.1	0.151	20.21
Ductus venosus	–	–	–	–	–	8.73
Syncytiotrophoblast	–	–	0.08	–	–	–
Amniotic fluid	–	–	0.758	–	–	–

[a] Physiologic parameters used in the nonpregnant PBPK model with arm sampling site model for a 66.8 kg nonpregnant individual were adopted from (Huang and Isoherranen, 2020).
[b] Physiologic parameters used in the maternal-fetal PBPK model for a 75.2 kg pregnant woman and a 3.44 kg fetus were calculated from equations published in (Abduljalil et al., 2012) and (Zhang et al., 2017b).

studies did not specify the sampling site, and comparison was done to the simulated plasma concentrations at the arm vein sampling site.

After validation of the PBPK model of alfentanil, an epidural dosing model was developed for alfentanil. The $CL_{pd,adipose}$ of alfentanil was extrapolated to be 0.01 l/h by multiplying the observed Caco-2 permeability of alfentanil at pH 7.4 (P_{app} = 300 × 10^{-6} cm/s) and the surface area of the epidural adipose tissue estimated based on the reported anatomic dimension of the epidural fat in the lumbar region (8.6 cm^2) (Reina et al., 2009). The K_p of the epidural adipose tissue was assumed to be the same as the rest of the adipose tissue in the body (K_p = 2.1). The f_u in the epidural fluid was assumed to be 1. The $CL_{pd,vein}$ was optimized from 0.01 l/h (same as $CL_{pd,adipose}$) to 0.3 l/h and validated using the observed mean plasma concentration-time profiles in healthy subjects from two epidural dosing studies of alfentanil (Coda et al., 1995, 1999) (Table 2). Simulations of alfentanil plasma concentration-time profiles after epidural dose were performed using the nonpregnant PBPK model and the same dose and sampling from the arm vein as in the original studies.

All observed mean plasma concentrations throughout were digitized using WebPlotDigitizer (version 4.3, https://apps.automeris.io/wpd/). The performance of all simulations was quantitatively evaluated based on the absolute average fold error (AAFE) calculated for each study according to eq. 1:

$$AAFE = 10^{\frac{1}{n}\sum\left|log_{10}\frac{Simulated\ concentration}{Observed\ concentration}\right|} \quad (1).$$

An AAFE of ≤2 was considered acceptable for the alfentanil model based on the interstudy variability of alfentanil CL observed in the above five intravenous dosing studies (CV = 17.4%). The 99.998% geometric confidence interval of the area under the plasma concentration-time curve was calculated according to (Abduljalil et al., 2014) to be 48% to 2.1-fold of the mean.

Validation of the Epidural Dosing Model of Fentanyl. To develop the epidural dosing PBPK model of fentanyl, a previously reported and validated PBPK model of fentanyl was adopted (Huang and Isoherranen, 2020) (Table 2). This model was previously validated for arterial and venous sampling of fentanyl after intravenous and buccal administration, defining the distribution parameters of fentanyl. The B/P ratio, f_u in plasma, and K_p's for fentanyl in different tissues were adopted as previously reported. The previous model only considered overall plasma CL in each study and it did not define the enzymatic pathways of fentanyl CL. Therefore, a hepatic clearance of fentanyl was calculated from the average observed plasma clearance (CL = 62 l/h) after intravenous administration of fentanyl to healthy subjects from four studies (McClain and Hug, 1980; Ziesenitz et al., 2015; Rauck et al., 2017; Nozari et al., 2019). Fentanyl renal clearance was set to an earlier reported value of 3 l/h (Ziesenitz et al., 2015). The $CL_{int,u}$ was back calculated from the mean hepatic clearance using the hepatic well stirred model resulting in an estimate of 1,055 l/h. Of the calculated $CL_{int,u}$, 80% was assumed to be mediated by CYP3A4 based on the result of a drug-drug interaction study (Ziesenitz et al., 2015) ($CL_{int,u,CYP3A4}$ = 844 l/h) and the remaining 20% was assigned to unknown pathways ($CL_{int,u,other}$ = 211 l/h). The modified fentanyl PBPK model was validated using the plasma concentrations observed in the above four intravenous studies. Simulations of fentanyl plasma concentration-time profiles after intravenous dose were performed using the nonpregnant PBPK model using the same dose and sampling site as specified in the original studies [three studies reported venous concentrations (Ziesenitz et al., 2015; Rauck et al., 2017; Nozari et al., 2019) and one study reported arterial concentrations (McClain and Hug, 1980)]. An acceptable AAFE was decided based on the interstudy variability of fentanyl CL observed in the above mentioned four intravenous studies (CV = 22.0%). The 99.998% geometric confidence interval of the area under the plasma concentration-time curve was calculated according to (Abduljalil et al., 2014) to be 40% to 2.5-fold of the mean. Therefore, an AAFE of ≤2 was used as an acceptance criterion for validation of the fentanyl model.

After validation of the PBPK model of fentanyl after intravenous dosing, the epidural dosing model of fentanyl was developed and validated using the observed plasma concentration-time profiles after epidural dosing in healthy subjects from two studies (Badner et al., 1990; Ginosar et al., 2003). The K_p of the epidural adipose tissue was assumed to be the same as the rest of the adipose tissue in the body. The f_u in the epidural fluid was assumed to be 1. The $CL_{pd,adipose}$ and $CL_{pd,vein}$ of fentanyl were scaled from the observed Caco-2 permeability of fentanyl at pH 7.4 (P_{app} = 35 × 10^{-6} cm/s) (Yu et al., 2018) using alfentanil as a scaler, a similar scaling approach as previously described for placental passive

TABLE 2

Physicochemical and pharmacokinetic parameters of alfentanil and fentanyl used in the PBPK models

Parameter[a]	Alfentanil	Fentanyl
Physicochemical properties		
MW (g/mol)	416.52	336.47
logP	2.16	4.05
pKa	6.5	8.99
B/P ratio	0.55	1
$f_{u,plasma}$	0.1	0.16[b]
*$f_{u,umbiliaclplasma}$	–	0.14
$f_{u,epiduralfluid}$	1	1
*$f_{u,syncytiotrophoblast}$	–	1
*$f_{u,amnioticfluid}$	–	1
Tissue partitioning coefficient (K_p)[c]		
Adipose	2.1	26.7
Bone	0.1	1
Brain	0.13	3.5
Gut	2.12	8.4
Heart	0.55	4.5
Kidney	0.82	12.1
Liver	1	3.8
Lung	0.78	13.5
Muscle	0.31	3.1
Skin	0.1	2.1
Spleen	0.73	27.6
Pancreas	0.96	21.3
Metabolism and excretion		
$CL_{int,u}$ (L/h)	185	1055
*CYP3A4 induction factor	–	1.99
CL_r (L/h)	1.3	3.3
*$CL_{syncytiotrophoblast}$ (L/h)	–	0
*Fetal hepatic $CL_{int,u}$ (L/h)	–	0.028[d]
Passive permeability clearance		
$CL_{pd,adipose}$ (L/h)	0.010	0.0012
$CL_{pd,vein}$ (L/h)	0.20	0.023
*$CL_{pd,placenta}$ (L/h)	–	357

CLr, renal clearance.

MF model specific parameters are marked with *.

[a] Alfentanil and fentanyl model parameters were collected from literature as described in the methods section.

[b] For nonpregnant population. Fentanyl $f_{u,plasma}$ in pregnant women was 0.12, measured in a group of 40 parturient women as described in the methods section.

[c] K_ps of alfentanil were adopted from values measured in rats (Bjorkman et al., 1990) as described in the methods section. K_p's of bone and skin were not reported and were assigned as 0.1 based on the observed V_{ss} of alfentanil (0.7 L/kg) in humans.

[d] Predicted from measured norfentanyl formation in FLM.

diffusion (Zhang and Unadkat, 2017). The $CL_{pd,adipose}$ and $CL_{pd,vein}$ of fentanyl for the epidural site were scaled using eq. 2:

$$CL_{pd,fentanyl} = CL_{pd,alfentanil} \times \frac{P_{app,fentanyl}}{P_{app,alfentanil}} \quad (2).$$

The $CL_{pd,adipose}$ and $CL_{pd,vein}$ of fentanyl were scaled to be 0.0012 and 0.023 l/h, respectively. Simulations of fentanyl plasma concentration-time profiles after epidural dose were performed using the nonpregnant PBPK model at the same dose and sampling from the artery as in the original studies. An AAFE of ≤2 was considered acceptable as described above.

Metabolism of Fentanyl by Fetal Liver Microsomes and Recombinant CYP3A7 and In Vitro to In Vivo Extrapolation (IVIVE). Pooled FLM were prepared from 14 individual fetal livers (mixture of males and females) previously collected from healthy pregnancies with no known maternal drug use (Topletz et al., 2019). The estimated gestational age at the time of tissue collection ranged from 87 to 137 days. Fetal liver microsomes (FLM) were prepared and pooled as previously described (Shum and Isoherranen, 2021) and the microsomal pellets stored at −80°C until experiments. Stock solutions of fentanyl, norfentanyl, and deuterated norfentanyl-d_5 were purchased from Millipore Sigma (St Louis, MO). Norfentanyl formation kinetics was characterized in the pooled FLM and recombinant CYP3A7 supersomes purchased from Corning, Inc. (Corning, NY). All incubations were done in potassium phosphate buffer (pH 7.4) at 37°C in a shaking water bath under conditions of protein and time linearity. Fentanyl (2, 5, 15, 30 μM) was incubated with pooled FLM (0.2 mg/ml) and recombinant CYP3A7 (10 pmol/ml) for 15 minutes after reactions were initiated with 1 mM NADPH (or potassium phosphate buffer for no NADPH controls) and quenched by addition of four parts of ice-cold acetonitrile containing norfentanyl-d_5 as internal standard. Samples were vortexed briefly and centrifuged at 16,100*g* for 15 minutes. The supernatants were stored at −20°C until HPLC-MS/MS analysis.

Norfentanyl intrinsic formation clearance ($C L_{int}$) by pooled FLM or CYP3A7 was estimated through linear regression of product formation versus substrate concentration in which the slope of the line is the CL_{int} when substrate concentration is below the K_m (v = [S]*CL_{int}) as described previously for oxycodone metabolism with CYP3A (Shum and Isoherranen, 2021). The CL_{int}'s were reported as the arithmetic means of data generated on three different days. The $CL_{int,FLM}$ was scaled to the whole fetal liver CL_{int} at term through IVIVE by multiplying the $CL_{int,FLM}$ with the measured microsomal protein per gram of liver (17.8 ± 4.2 mg protein/g liver) and the estimated fetal liver weight at term (i.e., 129 g) (Zhang et al., 2017a) to be used in the mf-PBPK model.

HPLC-MS/MS Analysis. The HPLC-MS/MS method to quantify norfentanyl was modified from a previously reported method (Ghassabian et al., 2012). Briefly, norfentanyl concentrations were measured using an AB Sciex 6500 qTrap Q-LIT mass spectrometer (Foster City, CA) equipped with an Agilent 1290 Infinity II UHPLC (Santa Clara, CA) and a Phenomenex Kinetex EVO C18 LC column (2.6 μm, 100 × 2.1 mm) with a Phenomenex SecurityGuard EVO-C18 cartridge (sub-2 μm, 2.1 mm) (Torrance, CA). A 7-minute gradient was employed using (A) 0.1% formic acid in water and (B) 0.1% formic acid in acetonitrile at a flow rate of 0.35 ml/min. The analytes were detected by positive ion electrospray ionization. The MS/MS transitions monitored for quantification were m/z 233 > 84 for norfentanyl and m/z 238 > 84 for norfentanyl-d_5. The lower limit of quantitation of norfentanyl was 1 nM.

Development of the mf-PBPK Model of Fentanyl. After validation of the PBPK model with epidural dosing of fentanyl, the mf-PBPK model was applied to predict fentanyl disposition in pregnant women and the maternal-fetal disposition of fentanyl at term. The K_p's and B/P ratio of fentanyl were assumed to be the same as those validated using the nonpregnant model. The maternal and fetal plasma f_u were set as 0.12 and 0.14, respectively, as the mean f_u values reported in a group of 40 parturient women and their newborns (Fernando et al., 1997). Additional simulations were performed using the fetal plasma f_u values of 0.01 and 0.34 (observed range in the above study). The maternal hepatic $CL_{int,u}$ of fentanyl was predicted to be 1,891 l/h based on the built-in 1.99 induction factor for CYP3A4, and the reported calculated CL_{int} for CYP3A4 described in the above sections. The fetal $CL_{int,u}$ was scaled from the measured $CL_{int,FLM}$ described above. The syncytiotrophoblast metabolism ($CL_{syncytiotrophoblast}$) of fentanyl was assumed to be negligible (Table 2).

The unbound transplacental clearance ($CL_{pd,placenta}$) of fentanyl ($CL_{pd,placenta,fentanyl}$) was scaled using midazolam as the scaler as previously described (Zhang and Unadkat, 2017) using eq. 3:

$$CL_{pd,\,placenta,fentanyl} = CL_{pd,\,placenta,\;\;midazolam} \times \frac{P_{app,\;\;fantanyl}}{P_{app,\,midazolam}} \quad (3).$$

The $CL_{pd,placenta,midazolam}$ was previously estimated to be 500 l/h (Zhang and Unadkat, 2017) and the $CL_{pd,placenta,fentanyl}$ was scaled to be 357 l/h using the observed Caco-2 permeability at pH 7.4 of fentanyl (P_{app} = 35 × 10^{-6} cm/s) (Yu et al., 2018) and midazolam (P_{app} = 49 × 10^{-6} cm/s) (Zhang and Unadkat, 2017).

Validation of the mf-PBPK Model of Fentanyl and Simulation of Maternal-Fetal Disposition of Fentanyl. The mf-PBPK model of fentanyl was validated by comparing the simulated MV, UV, and umbilical arterial (UA) plasma fentanyl concentrations with the same dose and sampling site (Fig. 1) to the respective plasma concentration observed in seven PK studies (Desprats et al., 1991, 1995; Bader et al., 1995; Loftus et al., 1995; Moisés et al., 2005; De Barros Duarte et al., 2009; Haidl et al., 2018). These studies were performed in parturient women at the first two stages of labor, administered with either a bolus epidural injection or continuous infusion of fentanyl. Four out of the seven studies reported maternal venous plasma concentrations during labor (Desprats et al., 1991, 1995; Moisés et al., 2005; Haidl et al., 2018), and all seven studies reported MV, UV, and/or UA concentrations at delivery. The reported mean maternal plasma concentrations were digitized, except one study that reported individual plasma concentrations for which mean plasma concentrations were calculated from individual data. One of the seven studies reported individual MV

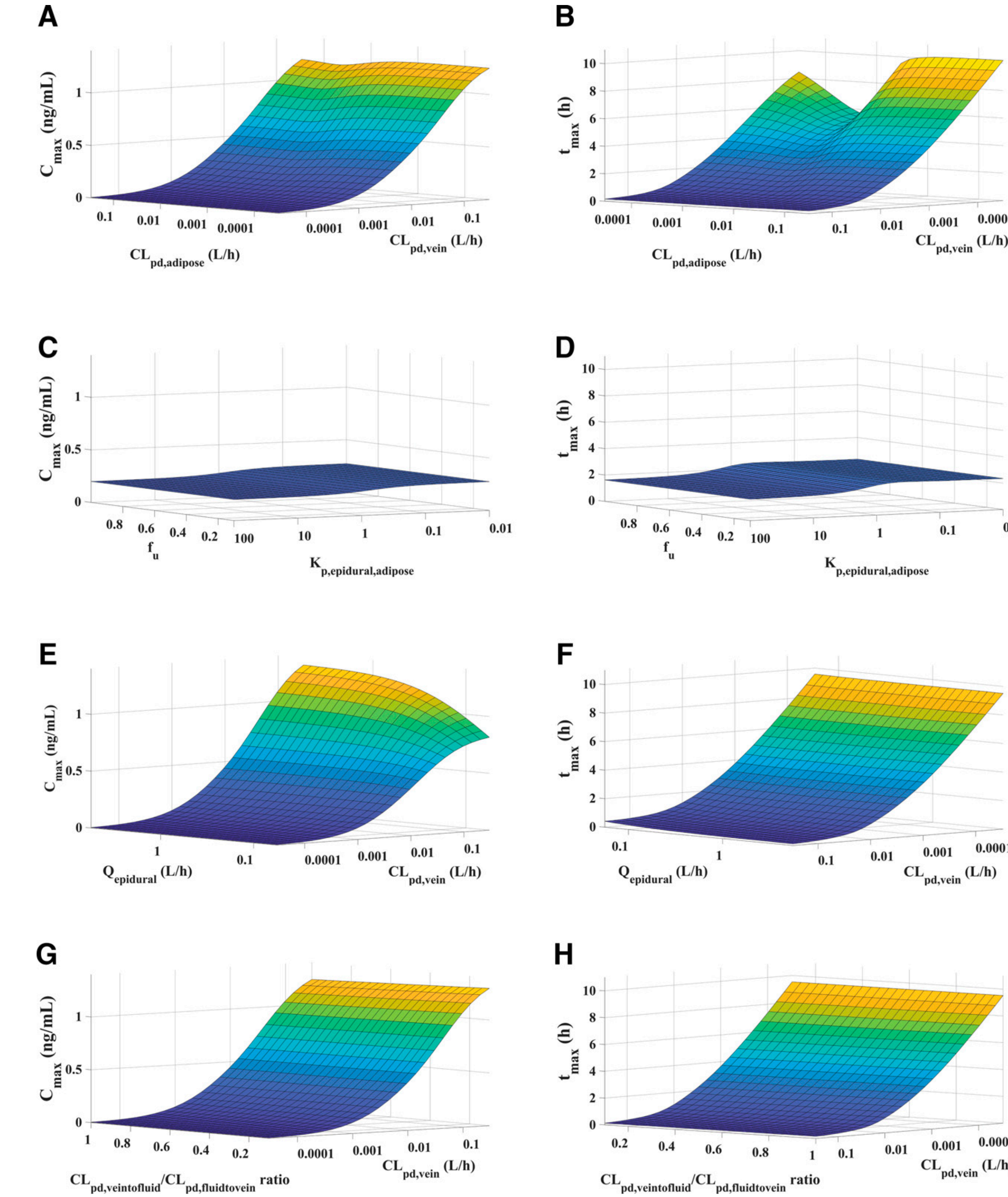

Fig. 2. Sensitivity analysis for epidural dosing site parameters of drug X. The effect of altered $CL_{pd,adipose}$ and $CL_{pd,vein}$ (ranging from 0.00003 to 0.3 l/h) on C_{max} and t_{max} of drug X is shown in (A) and (B). The impact of varying K_p (0.01 to 100) and f_u (0.1 to 1) (C and D), and the $Q_{epidural}$ (0.056 to 5.6 l/h) and $CL_{pd,vein}$ (0.00003 to 0.3 l/h) (E and F), and asymmetric $CL_{pd,vein}$ with $CL_{pd,fluidtovein}$ (10% to 100% of $CL_{pd,veintofluid}$) (G and H) on C_{max} and t_{max} of drug X are shown in (C–H). The parameters were kept constant unless stated otherwise ($CL_{pd,adipose}$ = 0.003 L/h, $CL_{pd,vein}$ = 0.003 l/h, K_p = 1, f_u = 1, $Q_{epidural}$ = 0.56 l/h). For comparison, the scales of the heat map for C_{max} and t_{max} were kept unchanged across the sensitivity analyses.

and UV concentrations at the time of delivery (Bader et al., 1995), and the reported concentrations were digitized. The AAFE was calculated by comparing the simulated and individual observed concentrations. For the remaining six studies, the mean delivery time and the mean MV, UV, and UA plasma concentrations were reported as numerical values and used as is. The absolute fold error was calculated by comparing the simulated concentration at the mean time of delivery with the mean observed plasma concentration at delivery. Since the interstudy variability of maternal-fetal disposition of fentanyl cannot be

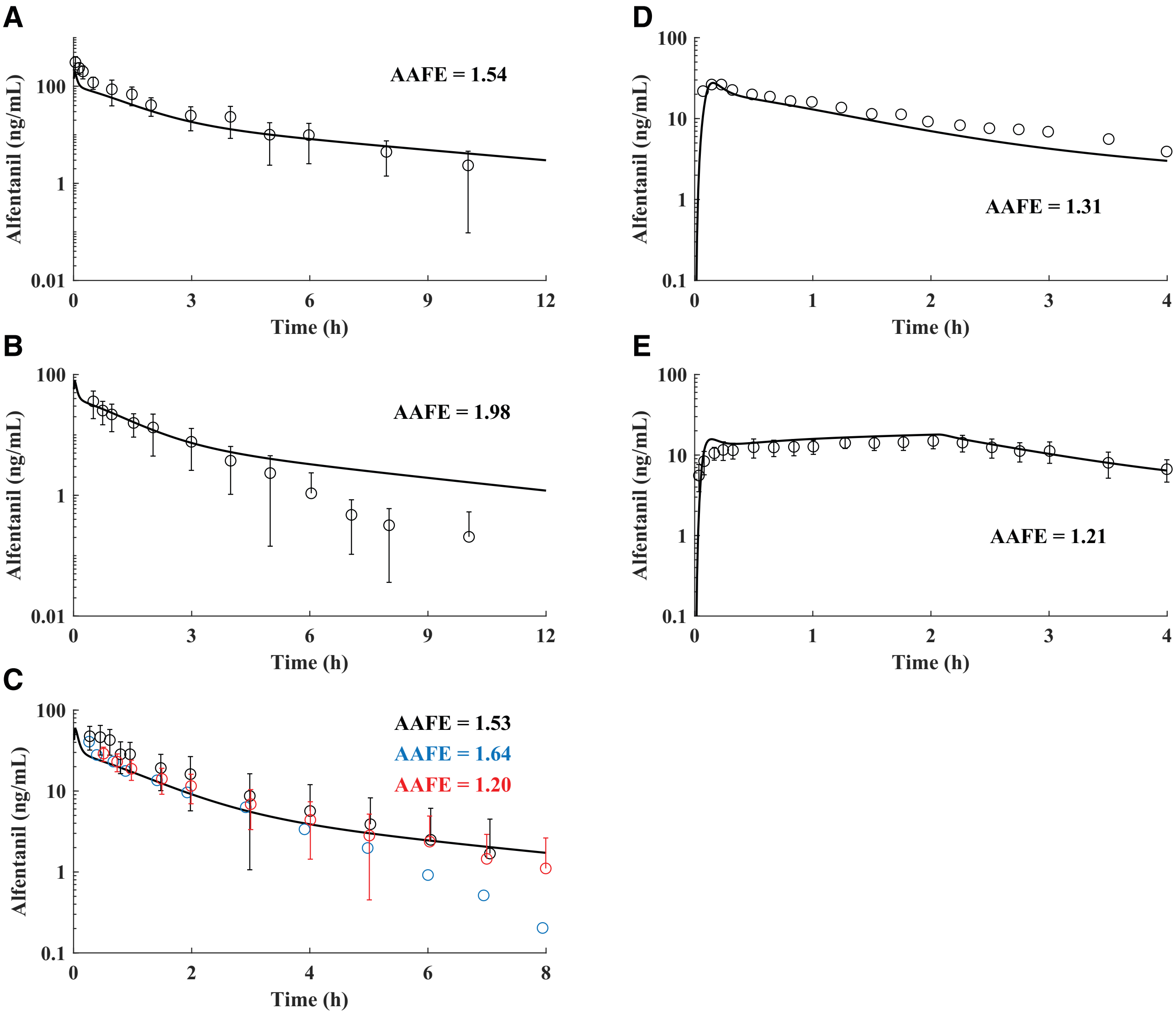

Fig. 3. Simulated plasma concentration-time profiles following intravenous and epidural administration of alfentanil using the nonpregnant PBPK model overlaid with mean observed plasma alfentanil concentrations in nonpregnant subjects. Simulated (solid lines) and mean observed (open circles) plasma concentrations from the arm vein following (A) a single intravenous bolus dose of 50 μg/kg (n = 10), (B) a single intravenous bolus dose of 20 μg/kg (n = 9), (C) a single intravenous bolus dose of 15 μg/kg (n = 6), (D) a single epidural dose of 750 μg (n = 7) and (E) a single epidural bolus dose of 400 μg plus an epidural infusion of 400 μg/h for 2 hours (n = 12). The mean observed fentanyl concentrations are from (Ferrier et al., 1985) (A), (Kharasch et al., 1997) (B), (Phimmasone and Kharasch, 2001) black circles, (Kharasch et al., 2004) blue circles, (Kharasch et al., 2011) red circles (C), (Coda et al., 1995) (D), and (Coda et al., 1999) (E). The error bars in (A–C) and (E) represent the S.D. as reported in the respective studies. The AAFE reported in each figure was calculated from the simulated and mean observed concentrations of each respective study.

estimated based on the available data, the same AAFE (≤2-fold) as the nonpregnant model was adopted as an acceptance criterion for validation of the fentanyl mf-PBPK model.

After validation of the mf-PBPK model of fentanyl, the maternal-fetal disposition of fentanyl at term was simulated after a single 500 μg intravenous bolus dose of fentanyl using the mf-PBPK model, and plasma fentanyl concentrations were sampled from the maternal artery (MA), MV, UV, and UA. The absolute concentrations and concentration ratios were assessed to explore potential fetal fentanyl exposures in cases of illicit use of fentanyl by pregnant women.

Results

Development of an Epidural Dosing Site Model. A novel epidural dosing site model was developed according to the physiology of the epidural space and incorporated into a full PBPK model to simulate drug disposition after epidural administration (Fig. 1). To evaluate the impact of physicochemical properties on drug disposition after epidural administration, sensitivity analyses were performed using the PBPK model of a hypothetical drug X (Fig. 2). First, the effect of apparent permeability (P_{app}) of drug X was tested by increasing $CL_{pd,adipose}$ and $CL_{pd,vein}$ (Fig. 2, A and B). The C_{max} of drug X increased by 282-fold, whereas the t_{max} decreased from 10 to 0.2 hours when $CL_{pd,vein}$ increased from 0.00003 to 0.3 l/h, suggesting that increasing P_{app} increases the rate of absorption after epidural administration and that $CL_{pd,vein}$ is a sensitive parameter in the model. In contrast, the C_{max} and t_{max} of drug X were relatively insensitive to changes in $CL_{pd,adipose}$. Second, the effect of increasing adipose tissue partitioning and increasing plasma f_u were tested (Fig. 2, C and D). The C_{max} and t_{max} of drug X were insensitive to changes in $K_{p,adipose}$ (increased from 0.01 to 100) and f_u (increased from 0.1 to 1), suggesting that sequestration of drug X in the adipose tissue and plasma protein

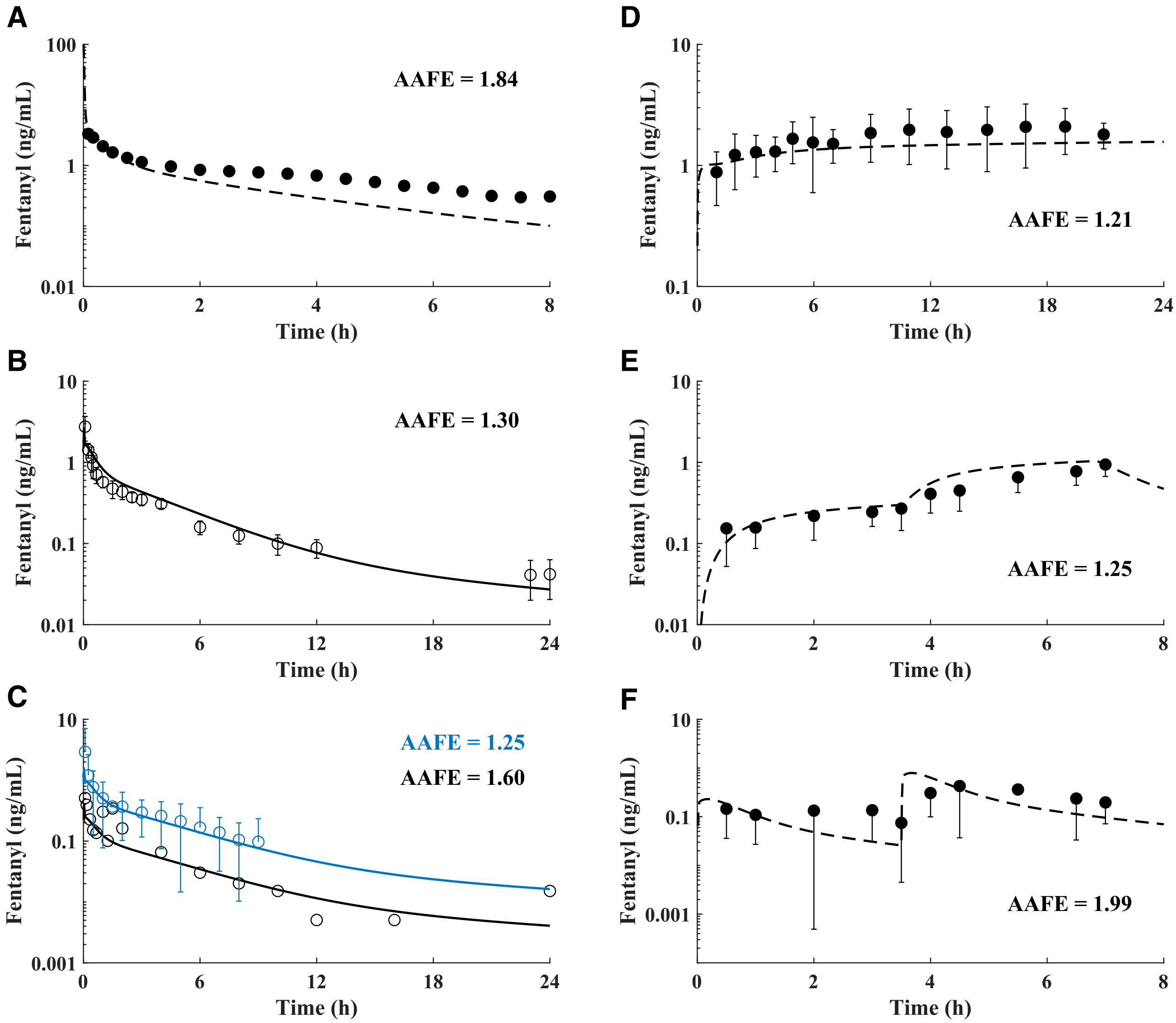

Fig. 4. Simulated plasma concentration-time profiles following intravenous and epidural administration of fentanyl using the nonpregnant PBPK model overlaid with mean observed plasma fentanyl concentrations in nonpregnant subjects. Simulated plasma concentrations from the arm vein (solid lines) and the artery (dashed lines), and the mean observed plasma concentrations from the arm vein (open circles) and the artery (closed circles) following (A) a single intravenous bolus dose of 6.4 µg/kg (n = 5), (B) a single intravenous bolus dose of 5 µg/kg (n = 16), (C) a single intravenous bolus dose of 50 µg (n = 10) in black, and a single intravenous bolus dose of 200 µg (n = 8) in blue, (D) an epidural bolus dose of 100 µg and continuous epidural infusion of 114.3 µg/h for 24 hours (n = 10), (E) epidural infusion at 30 µg/h for 3.5 hours and increased to 100 µg/h for another 3.3 hours (n = 10), and (F) an epidural bolus dose of 30 µg followed by a second epidural bolus dose of 100 µg at 3.5 hours (n = 10). The mean observed fentanyl concentrations are from (McClain and Hug, 1980) (A), (Ziesenitz et al., 2015) (B), (Rauck et al., 2017) and (Nozari et al., 2019) (C), (Badner et al., 1990) (D), and (Ginosar et al., 2003) (E and F). The error bars in (B–D) represent the S.D. and in (E) and (F) represent the 25th quartile as reported in the respective studies. The AAFE reported in each figure was calculated from the simulated and mean observed concentrations of each respective study.

binding have minimal effect on the rate of absorption after epidural administration. As such, neither $K_{p,adipose}$ nor f_u are sensitive parameters in the model. Third, the effect of decreasing epidural blood flow ($Q_{epidural}$ decreased from 5.6 to 0.056 l/h) was tested (Fig. 2, E and F). The C_{max} of drug X was not affected by decreasing $Q_{epidural}$ when $CL_{pd,vein}$ was low (<0.01 l/h, P_{app} = 3 × 10^{-4} cm/s), but C_{max} was sensitive to $Q_{epidural}$ under high $CL_{pd,vein}$ conditions. This suggests that the rate of absorption becomes limited by blood flow for drugs with a high P_{app}, and hence, correct parameterization for blood flow is important for high permeability compounds. Last, sensitivity analysis was performed to evaluate whether uptake through CSF to the venous system is kinetically discernable by introducing asymmetric $CL_{pd,fluidtovein}$ and $CL_{pd,veintofluid}$ (Fig. 2, G and H). The simulations showed that the C_{max} and t_{max} of drug X were not affected by the asymmetric $CL_{pd,vein}$ suggesting that an alternative route of drug absorption through the CSF is not kinetically discernable after epidural dosing.

Verification of the Epidural Dosing Model Using Alfentanil as the Model Compound. The epidural dosing site model was optimized and verified using alfentanil as the model drug. The final parameters of the alfentanil model are listed in Table 2. First, a PBPK model of alfentanil was developed to simulate the plasma concentration-time profile of alfentanil after intravenous administration to nonpregnant healthy subjects (Fig. 3, A–C). The simulated venous plasma concentration-time profiles captured the observed mean venous alfentanil plasma concentration-time profiles from five studies with intravenous dosing of alfentanil within the acceptance criterion (AAFE 1.20–1.98), validating the alfentanil model. Then, the $CL_{pd,vein}$ of alfentanil was optimized to 0.2 l/h based on the observed venous plasma concentration-time profile

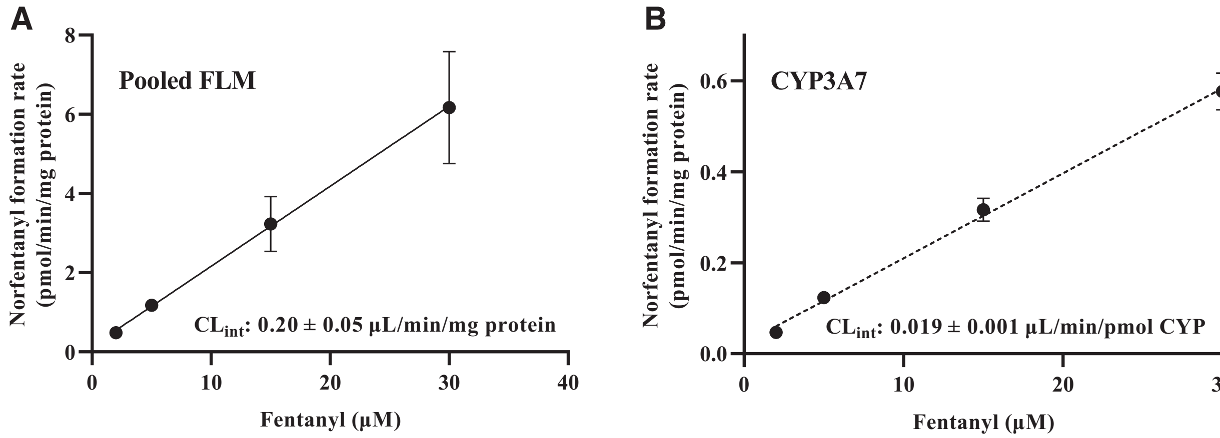

Fig. 5. Norfentanyl formation kinetics with pooled FLM (14 donors) and recombinant CYP3A7. Metabolite formation rate as a function of fentanyl concentration for norfentanyl formation by (A) pooled FLM and (B) CYP3A7. The CL_{int} values shown were estimated by linear regression. Mean and S.D. of CL_{int} reported were calculated from three different experiments conducted on separate days.

after epidural administration in nonpregnant healthy subjects reported in two epidural dosing studies (Fig. 3, D and E). The simulated plasma concentration-time profiles using the optimized PBPK model of alfentanil captured the observed mean alfentanil plasma concentration-time profiles after epidural dosing acceptably (AAFE: 1.21–1.31) validating the epidural dosing model.

Development and Validation of an Epidural Dosing Model of Fentanyl. After verification of the epidural dosing site model and validation of the alfentanil model, the fentanyl model for intravenous and epidural administration was developed and validated. First, a previously published (Huang and Isoherranen, 2020) fentanyl PBPK model was adopted and modified with refined hepatic clearance parameters reflecting the CYP3A4 intrinsic clearance (Table 2). The fentanyl model was validated using the mean venous plasma concentrations observed in three studies and the mean arterial plasma concentrations observed in one study after intravenous dosing of fentanyl (Fig. 4, A–C). All simulations met the acceptance criterion of AAFE $\leq$2 (AAFE: 1.25–1.84) when compared with the observed data validating the fentanyl model. Then, the epidural dosing model of fentanyl was developed using alfentanil as a scaler. The simulated plasma concentration-time profiles after epidural administration of fentanyl to healthy nonpregnant subjects captured the observed venous plasma concentration-time profiles (Fig. 4, D–F) with all AAFEs within the acceptance criteria of $\leq$2 (AAFE: 1.21–1.99) validating the epidural dosing model of fentanyl in nonpregnant women.

FLM Metabolism of Fentanyl and IVIVE to Predict Fetal Hepatic Intrinsic Clearance. Fentanyl is mainly metabolized by CYP3A4 to norfentanyl in the adult liver (Labroo et al., 1997), and we hypothesized that fentanyl is also a substrate for CYP3A7 in the fetal liver. To test this hypothesis, norfentanyl formation was measured with recombinant CYP3A7 and in FLM. Norfentanyl was formed from fentanyl by recombinant CYP3A7 with CL_{int} of 0.019 ± 0.001 µl/min/pmol cytochrome P450 (Fig. 5). Using the previously established intersystem extrapolation factor of 0.044 for CYP3A7 and the measured CYP3A7 expression in the pooled FLM (359 pmol/mg protein) (Shum and Isoherranen, 2021), norfentanyl formation CL_{int} was predicted to be 0.3 µl/min/mg protein in FLM. The formation CL_{int} of norfentanyl in FLM (0.20 ± 0.05 µl/min/mg protein) was 0.7-fold of the predicted CL_{int} (Fig. 5), suggesting that CYP3A7 is the main enzyme responsible for norfentanyl formation in the fetal liver. The measured norfentanyl formation CL_{int} in FLM was used to predict the fetal hepatic $CL_{int,u}$ resulting in a predicted fetal hepatic $CL_{int,u}$ of 0.028 l/h. This $CL_{int,u}$ was incorporated in the fetal liver of the mf-PBPK model of fentanyl (Table 2).

Validation of the mf-PBPK Model of Fentanyl and Simulations of Fentanyl Disposition. The developed mf-PBPK model of fentanyl was validated by comparing simulated MV plasma concentrations and UV and UA concentrations to available observed data after epidural bolus or epidural infusion of fentanyl (Fig. 6). The simulations captured the observed maternal plasma concentration-time profiles (AAFE 1.18–1.86) and the observed UV (AAFE: 1.15–2.36) and UA (AAFE: 1.3–1.65) concentrations within the reported time window of sampling. Several studies also reported the UV/MV (Desprats et al., 1991, 1995; Moisés et al., 2005; De Barros Duarte et al., 2009) and UA/UV (Desprats et al., 1991) plasma fentanyl concentration ratios at the time of delivery. To compare the simulated ratios to the observed ratios as a function of time following a single epidural bolus dose, the UV/MV and UA/UV ratios were calculated using the simulated plasma concentrations following a single epidural bolus dose of 100 µg fentanyl and compared with the observed data (Fig. 7). The simulations show that the concentration ratios vary with time, particularly the UV/MV ratio that rises rapidly over the initial few minutes following dosing to about 2.6 and then gradually declines to $<$1 at around 30 minutes, capturing the variability of the observed UV/MV ratios of 0.43–0.89 at around 30 minutes postdose reported in the above studies. To further explore the time course of maternal-fetal distribution of fentanyl, the UV/MA ratio was also calculated using the simulated UV and MA plasma concentrations (Fig. 7). In contrast to the UV/MV ratio, the UV/MA ratio gradually increases with time to 0.7 at 2 hours postdose.

The validated mf-PBPK model of fentanyl was then used to simulate the maternal (MA and MV) and fetal (UV and UA) plasma concentration-time profiles in pregnant women following a single intravenous bolus dose of 500 µg fentanyl to explore the maternal-fetal disposition of fentanyl in a potential drug abuse scenario (Fig. 8A). The simulated C_{max} of MA, MV, UV, and UA were 150, 3.9, 11, and 2.0 ng/ml, respectively. Similar to the simulated concentration ratios following epidural bolus dose, the UV/MV ratio was predicted to rise above 3 in the initial minutes following an intravenous bolus dose and gradually decline to $<$1 at around 15 minutes postdose (Fig. 8B). Notably, the UV/UA ratio also increased with time approaching 1 at 2 hours after dosing.

Discussion

In recent years, there has been an increasing interest to use mf-PBPK modeling to study maternal-fetal disposition of xenobiotics because of

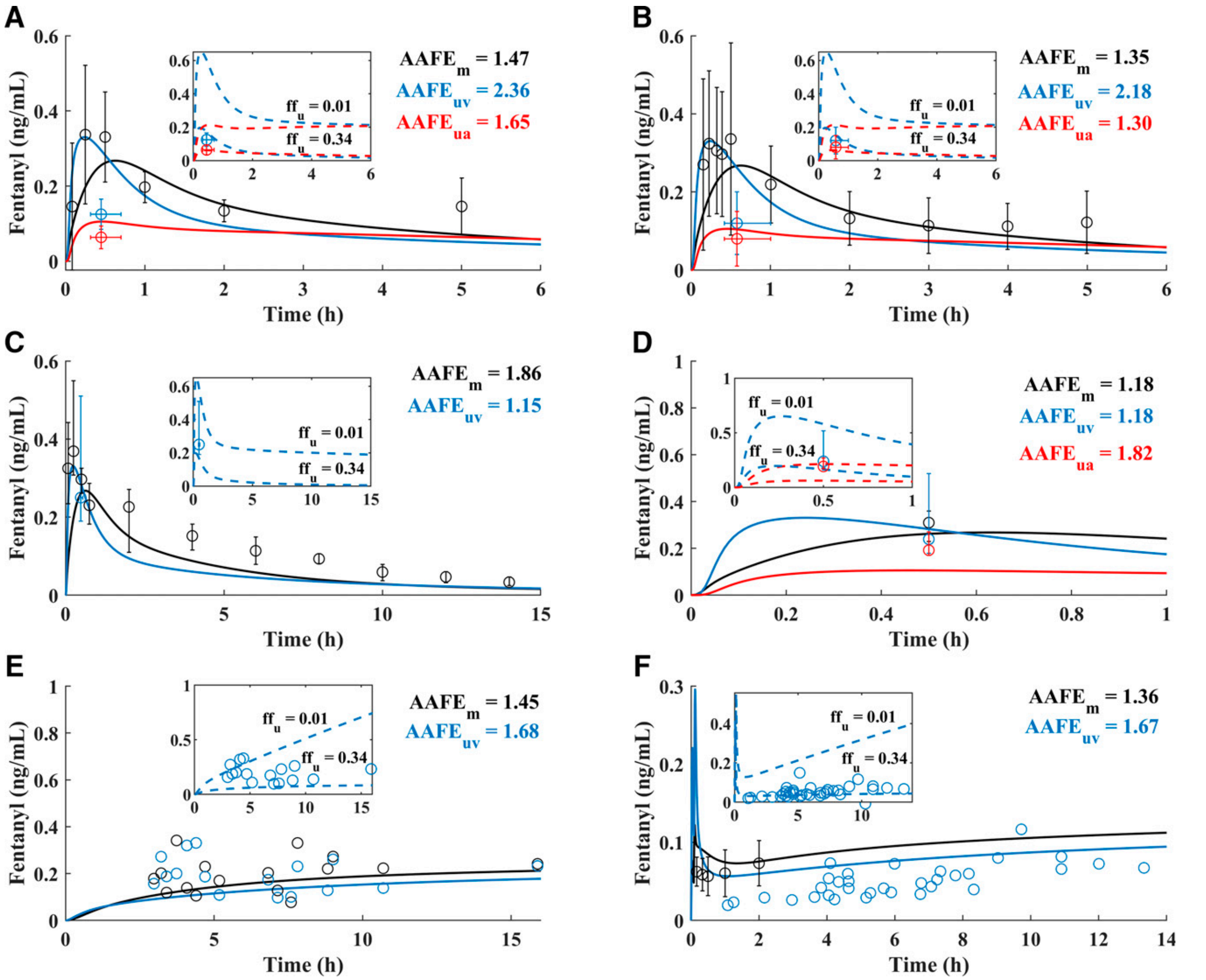

Fig. 6. Simulated maternal venous (m), UV, and UA plasma concentration-time profiles following epidural administration of fentanyl overlaid with observed plasma concentrations. The simulated (black solid lines) and observed (black open circles) m concentrations, simulated (blue solid lines) and observed (blue open circles) UV concentrations, and simulated (red solid lines) and observed (red open circles) UA concentrations following (A) a single epidural bolus dose of 100 μg fentanyl (n = 16), (B) a single epidural bolus dose of 100 μg fentanyl (n = 16), (C) a single epidural bolus dose of 100 μg fentanyl (n = 10), (D) a single epidural bolus dose of 100 μg fentanyl (n = 10), (E) continuous 20 μg/h infusion of fentanyl (n = 21), and (F) two bolus doses of 10 μg fentanyl and continuous 10 μg/h infusion of fentanyl (n = 19). The observed fentanyl concentrations are from (Desprats et al., 1991) (A), (Desprats et al., 1995) (B), (Moisés et al., 2005) (C), (de Barros Duarte et al., 2009) (D), (Bader et al., 1995) (E), and (Haidl et al., 2018) (F). The AAFE reported in (A–D) and (F) (m only) were calculated from the simulated and the mean observed m, ua, uv concentrations at each timepoint of each respective study. The AAFE reported in (E) and (F) (UV only) were calculated from the simulated and observed concentration of each individual subject. The Y-axis error bars in (A and B) and (F) represent the S.D. and in (C and D) represent the 25th and 75th quartile as reported in the respective studies. (E) shows the simulated m and UV concentrations (solid lines) in comparison with individual subject data at delivery (open circles) and (F) shows the simulated UV (blue solid line) and observed individual subject uv concentrations at delivery (blue open circles). The X-axis error bars in panels (A–C) represent the window of the reported sampling time (i.e., time of delivery). Insets in all panels show the simulated UV (dashed blue lines) and UA (dashed red lines) plasma concentrations with unbound fraction in fetal plasma (ff_u) of 0.01 and 0.34 illustrating the impact of plasma protein binding on umbilical cord concentrations and observed concentrations.

the ethical concerns and challenges in conducting clinical pharmacokinetic studies in pregnant women (Ke et al., 2014, 2018). Fentanyl is of particular interest (Fleet et al., 2011) because it is used to manage pain during labor and delivery and it is an opioid abused by pregnant women. The fetal disposition of fentanyl and alternative opioid analgesics is of interest to better predict, prevent, and manage fetal side effects of opioids. However, information on the fetal disposition of fentanyl is limited to measurements of single timepoint UV/MV ratios at time of delivery. Moreover, the reported UV/MV ratios appear to be dependent on the sampling time postdose due to distribution kinetics, which makes it difficult to assess overall fetal exposure. We used mf-PBPK modeling to simulate maternal and fetal disposition of fentanyl to define fetal exposures to fentanyl after various routes of administration and to establish a modeling and simulations workflow that could be used for other drugs administered to pregnant women.

To simulate the maternal-fetal disposition of fentanyl following epidural dose, an epidural PBPK model was developed. Drug absorption following epidural administration is a complex process because of the unique physiology of the epidural space. The sensitivity analyses using a hypothetical drug X demonstrated that $CL_{pd,vein}$ is the major rate-determining factor of drug absorption following epidural injection. Since there is currently no information on the surface area of the

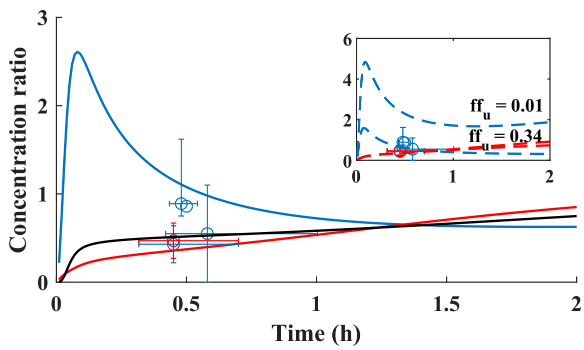

Fig. 7. Simulated maternal to umbilical vein and artery plasma concentration ratio-time profiles following an epidural bolus dose of 100 µg fentanyl overlaid with observed concentration ratios. The simulated (blue line) and observed (blue open circles) umbilical venous/maternal venous (UV/MV) concentration ratios, the simulated (red line) and observed (red open circles) umbilical arterial/umbilical venous (UA/UV) concentration ratios, and the simulated (black line) umbilical venous/maternal arterial (UV/MA) concentration ratios over time (0–2h) following a single epidural bolus dose of 100 µg fentanyl. The observed ratios are from (Desprats et al., 1991) (n = 16), (Desprats et al., 1995) (n = 16), (Moisés et al., 2005) (n = 10), and (de Barros Duarte et al., 2009) (n = 10). The Y-axis error bars represent the S.D. or the 25^{th}–75^{th} percentile and the X-axis error bars represent the window of the reported sampling time (i.e., time of delivery). Insets show the simulated UV/MV (dashed blue lines) and UA/UV (dashed red lines) ratios with unbound fraction in fetal plasma (ff_u) of 0.01 and 0.34 and observed ratios.

epidural venous system, the $CL_{pd,vein}$ of fentanyl was defined using a scaler compound alfentanil. The observed Caco-2 permeability for alfentanil and fentanyl together with alfentanil optimized $CL_{pd,vein}$ were deployed in accordance to a method previously established to predict transplacental clearance (Zhang and Unadkat, 2017). The optimized $CL_{pd,vein}$ was 20-fold higher than the estimated $CL_{pd,adipose}$ scaled based on the surface area of the adipose tissue likely reflecting higher barrier permeability due to larger venous surface area and fenestration in the blood vessels (Becske and Nelson, 2009). The scaling approach yielded a fentanyl model that successfully simulated fentanyl PK after epidural dosing. This suggests that epidural absorption kinetics is directly governed by endothelial permeability, and that this method and the developed epidural dosing model can be used more broadly for other drugs and for dosing in nonpregnant individuals to aid in the design of dosing strategies. The model can also be coupled with a pharmacodynamic (PD) model to allow PK-PD simulations for pain management.

Fetal liver metabolism of fentanyl has been suggested based on the high CYP3A4 mediated hepatic $CL_{int,u}$ of fentanyl observed in adults (Labroo et al., 1997) and similar substrate specificity of CYP3A4 and CYP3A7 (Williams et al., 2002). However, no metabolism of fentanyl by CYP3A7 has been reported. This study showed that both CYP3A7 and pooled FLM metabolize fentanyl to norfentanyl, the major fentanyl metabolite formed by CYP3A4 in adults. Fentanyl metabolism in FLM is likely mediated by CYP3A7 based on the extrapolation from supersomes to FLM using a measured CYP3A7 expression and established intersystem extrapolation factor for CYP3A7. The extrapolated fetal hepatic $CL_{int,u}$ (0.028 l/h) was significantly less than the observed adult hepatic $CL_{int,u}$ (1,055 l/h), and the predicted extraction ratio by fetal liver was very low, <0.01. Although it is possible that the predicted fetal hepatic $CL_{int,u}$ is an underprediction of the the $CL_{int,u}$, such underprediction would be unlikely to affect the overall simulations. Even if the predicted $CL_{int,u}$ is only 10% of the in vivo $CL_{int,u}$, the fetal liver is unlikely to quantitatively contribute to the maternal-fetal clearance of fentanyl. Moreover, the fetal hepatic $CL_{int,u}$ is low in comparison with fetal hepatic blood flow and transplacental clearance, suggesting that fetal liver metabolism does not affect fetal drug disposition. The minor role of fetal liver metabolism was also confirmed through the simulations using the mf-PBPK model that the UA/UV ratio was unity following epidural infusion to steady state.

The simulations undertaken to explore fetal exposure to fentanyl after intravenous bolus dose (500 µg) that may occur in drug abuse scenarios show that fetal fentanyl concentrations are likely to reach pharmacologically active concentrations that may cause a risk to the fetus. The simulated total C_{max} of fentanyl in UV was ~33nM (11 ng/ml), a concentration that exceeds the reported fentanyl EC_{50} (20–24 nM) (Lötsch, 2005; Kalvass et al., 2007). However, the umbilical cord plasma protein binding had a significant impact on the concentrations simulated in UV and UA. As the values reported in the literature for fentanyl protein binding in the umbilical cord vary considerably, these simulations suggest that more data are needed regarding fentanyl protein binding in fetal circulation.

The simulations of maternal-fetal disposition of fentanyl illustrate an important concept that the umbilical venous and arterial concentrations (commonly collected to reflect fetal exposure) and the maternal arterial and venous concentrations and their ratios following a bolus dose depend on the distribution kinetics in the mom, fetus, and across the placenta. The UV/MV ratio is most commonly reported in clinical studies to reflect the transplacental transfer from the mom to the fetus, but the results of the simulations shown here demonstrate that this ratio can be very misleading and confound interpretation of maternal-fetal distribution if measured under nonsteady-state circumstances and based on a

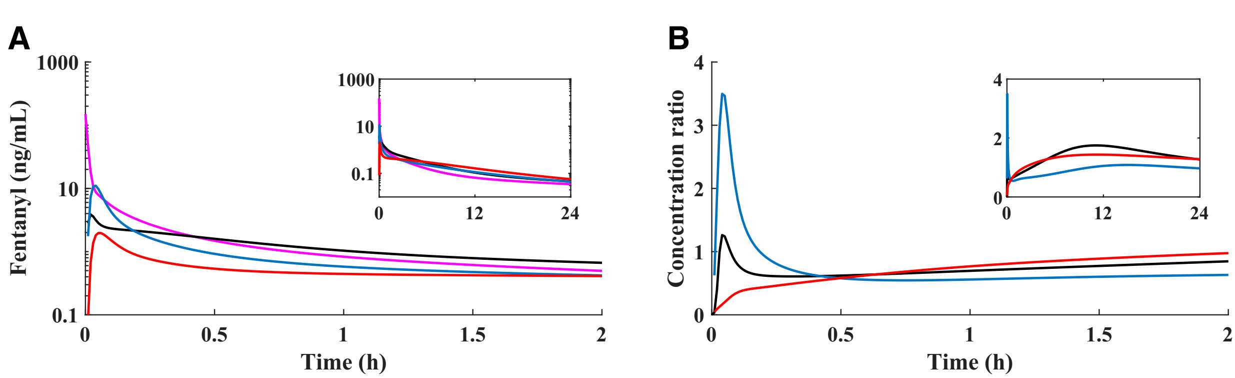

Fig. 8. Simulated maternal and umbilical cord fentanyl plasma concentrations and concentration ratios following a single IV bolus dose of 500 µg fentanyl using the validated mf-PBPK model. (A) shows the simulated MA (solid magenta line), MV (solid black line), UV (solid blue line), and UA (solid red line) plasma concentration-time profiles (0–2h) following a single intravenous bolus dose of 500 µg fentanyl. (B) shows the UV/MA (solid black line), UV/MV (solid blue line), and UA/UV (solid red line) ratio-time profile of the simulated plasma concentrations. The insets show the simulated data until 24 hours after dosing.

single time point. The simulations also illustrate that time dependent variation in UV/MV ratio likely explains the variability in experimentally measured values. Physiologically, the placenta is perfused with maternal arterial blood instead of venous blood, and hence, the maternal arterial blood concentration is the main driver of the distribution kinetics across the placenta (i.e., syncytiotrophoblast monolayer). Depending on the PK properties of the drug, the arteriovenous concentration difference in the mom could be large (Huang and Isoherranen, 2020), resulting in very different UV/MV and UV/MA concentration ratios. The arteriovenous concentration difference of fentanyl was captured by these simulations and is also supported by the observed 2-fold higher placental intervillous space plasma fentanyl concentration (maternal side) (2.02 nM) compared with the MV plasma concentration (0.92 nM) at about 30 minutes post epidural bolus dose (De Barros Duarte et al., 2009). Hence, the high UV/MV ratio of fentanyl does not reflect a rapid transplacental transfer, but rather the arteriovenous distribution kinetics in the mother, and hence can be misleading for assessing fetal exposure to fentanyl. As illustrated by the UV/MA ratio, the transplacental distribution of fentanyl to the fetus is relatively slow taking several hours to reach distribution equilibrium. Notably, the simulated UV/MA ratios were different than the commonly reported UV/MV ratios, in particular during the earlier time points suggesting the potential for systematic errors in assessing transplacental permeability from UV/MV ratios.

The UA/UV ratio reflects the distribution kinetics (and metabolism) in the fetus. The UV concentration is the concentration on the fetal side of the placenta after the drug crosses the placenta and before fetal distribution and metabolism. The UA concentration is the fetal arterial concentration after fetal distribution and metabolism. The UA/UV ratio following a bolus dose of fentanyl suggest that the fetal distribution of fentanyl is slow, as distribution equilibrium was not reached until 30 hours postdose. The data presented suggests that to best capture maternal-fetal distribution and potential fetal clearance, steady-state concentration ratios should be measured. An early measurement of UA/UV ratio that is $\ll 1$ could be misinterpreted to imply metabolism in the fetus.

In conclusion, our study demonstrates that maternal-fetal disposition of drugs can be predicted using mf-PBPK modeling, and this tool can be used to study maternal-fetal disposition of drugs that are difficult to study in the clinic. The simulations using the mf-PBPK model illustrate that the umbilical cord/maternal plasma concentration ratio is significantly impacted by maternal, fetal, and transplacental distribution kinetics after a bolus dose. Any fetal-maternal concentration ratios should be interpreted with caution, as they must take into account the time course of drug distribution which can be accomplished through mf-PBPK modeling.

Acknowledgments

The authors wish to thank Dr. Evan Kharasch for helpful discussions during this work.

Authorship Contributions

Participated in research design: Shum, Shen, and Isoherranen.

Conducted experiments: Shum.

Performed data analysis: Shum.

Wrote or contributed to the writing of the manuscript: Shum, Shen, and Isoherranen.

References

Abduljalil K, Cain T, Humphries H, and Rostami-Hodjegan A (2014) Deciding on success criteria for predictability of pharmacokinetic parameters from in vitro studies: an analysis based on in vivo observations. *Drug Metab Dispos* **42**:1478–1484.

Abduljalil K, Furness P, Johnson TN, Rostami-Hodjegan A, and Soltani H (2012) Anatomical, physiological and metabolic changes with gestational age during normal pregnancy: a database for parameters required in physiologically based pharmacokinetic modelling. *Clin Pharmacokinet* **51**:365–396.

Arslan M, Comert A, Acar HI, Ozdemir M, Elhan A, Tekdemir I, Tubbs RS, and Ugur HC (2011) Surgical view of the lumbar arteries and their branches: an anatomical study. *Neurosurgery* **68**(1, Suppl Operative)16–22, discussion 22.

Bader AM, Fragneto R, Terui K, Arthur GR, Loferski B, and Datta S (1995) Maternal and neonatal fentanyl and bupivacaine concentrations after epidural infusion during labor. *Anesth Analg* **81**:829–832.

Badner NH, Sandler AN, Koren G, Lawson SL, Klein J, and Einarson TR (1990) Lumbar epidural fentanyl infusions for post-thoracotomy patients: analgesic, respiratory, and pharmacokinetic effects. *J Cardiothorac Anesth* **4**:543–551.

Baxter AD, Laganière S, Samson B, Stewart J, Hull K, and Goernert L (1994) A comparison of lumbar epidural and intravenous fentanyl infusions for post-thoracotomy analgesia. *Can J Anaesth* **41**:184–191.

Becske T and Nelson PK (2009) The vascular anatomy of the vertebro-spinal axis. *Neurosurg Clin N Am* **20**:259–264.

Bernards CM, Shen DD, Sterling ES, Adkins JE, Risler L, Phillips B, and Ummenhofer W (2003) Epidural, cerebrospinal fluid, and plasma pharmacokinetics of epidural opioids (part 1): differences among opioids. *Anesthesiology* **99**:455–465.

Björkman S, Stanski DR, Verotta D, and Harashima H (1990) Comparative tissue concentration profiles of fentanyl and alfentanil in humans predicted from tissue/blood partition data obtained in rats. *Anesthesiology* **72**:865–873.

Bower S and Hull CJ (1982) Comparative pharmacokinetics of fentanyl and alfentanil. *Br J Anaesth* **54**:871–877.

Buffington CW, Nichols L, Moran PL, and Blix EUM (2011) Direct connections between the spinal epidural space and the venous circulation in humans. *Reg Anesth Pain Med* **36**:134–139.

Coda BA, Brown MC, Risler L, Syrjala K, and Shen DD (1999) Equivalent analgesia and side effects during epidural and pharmacokinetically tailored intravenous infusion with matching plasma alfentanil concentration. *Anesthesiology* **90**:98–108.

Coda BA, Brown MC, Schaffer RL, Donaldson G, and Shen DD (1995) A pharmacokinetic approach to resolving spinal and systemic contributions to epidural alfentanil analgesia and side-effects. *Pain* **62**:329–337.

de Barros Duarte L, Moisés EC, Carvalho Cavalli R, Lanchote VL, Duarte G, and da Cunha SP (2009) Distribution of fentanyl in the placental intervillous space and in the different maternal and fetal compartments in term pregnant women. *Eur J Clin Pharmacol* **65**:803–808.

Desjardins AE, Hendriks BHW, van der Voort M, Nachabé R, Bierhoff W, Braun G, Babic D, Rathmell JP, Holmin S, Söderman M, et al. (2011) Epidural needle with embedded optical fibers for spectroscopic differentiation of tissue: ex vivo feasibility study. *Biomed Opt Express* **2**:1452–1461.

Desprats R, Dumas JC, Giroux M, Campistron G, Faure F, Teixeira MG, Grandjean H, Houin G, and Pontonnier G (1991) Maternal and umbilical cord concentrations of fentanyl after epidural analgesia for cesarean section. *Eur J Obstet Gynecol Reprod Biol* **42**:89–94.

Desprats R, Giroux M, Dumas JC, Campistron G, Teixeira MG, Houin G, and Grandjean H (1995) Effect of adrenaline on plasma concentrations of fentanyl during epidural anaesthesia for caesarean section. *Int J Obstet Anesth* **4**:225–229.

Ellis DJ, Millar WL, and Reisner LS (1990) A randomized double-blind comparison of epidural versus intravenous fentanyl infusion for analgesia after cesarean section. *Anesthesiology* **72**:981–986.

Espahbodi S, Doré CJ, Humphries KN, and Hughes SPF (2013) Color Doppler ultrasonography of lumbar artery blood flow in patients with low back pain. *Spine* **38**:E230–E236.

Fernando R, Bonello E, Gill P, Urquhart J, Reynolds F, and Morgan B (1997) Neonatal welfare and placental transfer of fentanyl and bupivacaine during ambulatory combined spinal epidural analgesia for labour. *Anaesthesia* **52**:517–524.

Ferrier C, Marty J, Bouffard Y, Haberer JP, Levron JC, and Duvaldestin P (1985) Alfentanil pharmacokinetics in patients with cirrhosis. *Anesthesiology* **62**:480–484.

Fleet J, Jones M, and Belan I (2011) Non-axial administration of fentanyl in childbirth: a review of the efficacy and safety of fentanyl for mother and neonate. *Midwifery* **27**:e106–e113.

Ghassabian S, Moosavi SM, Valero YG, Shekar K, Fraser JF, and Smith MT (2012) High-throughput assay for simultaneous quantification of the plasma concentrations of morphine, fentanyl, midazolam and their major metabolites using automated SPE coupled to LC-MS/MS. *J Chromatogr B Analyt Technol Biomed Life Sci* **903**:126–133.

Ginosar Y, Riley ET, and Angst MS (2003) The site of action of epidural fentanyl in humans: the difference between infusion and bolus administration. *Anesth Analg* **97**:1428–1438.

Grangier L, Martinez de Tejada B, Savoldelli GL, Irion O, and Haller G (2020) Adverse side effects and route of administration of opioids in combined spinal-epidural analgesia for labour: a meta-analysis of randomised trials. *Int J Obstet Anesth* **41**:83–103.

Haas DM, Marsh DJ, Dang DT, Parker CB, Wing DA, Simhan HN, Grobman WA, Mercer BM, Silver RM, Hoffman MK, et al. (2018) Prescription and other medication use in pregnancy. *Obstet Gynecol* **131**:789–798.

Haidl F, Rosseland LA, Spigset O, and Dahl V (2018) Effects of adrenaline on maternal and fetal fentanyl absorption in epidural analgesia: A randomized trial. *Acta Anaesthesiol Scand* **62**:1267–1273.

Haight SC, Ko JY, Tong VT, Bohm MK, and Callaghan WM (2018) Opioid use disorder documented at delivery hospitalization - United States, 1999-2014. *MMWR Morb Mortal Wkly Rep* **67**:845–849.

Hebert MF, Easterling TR, Kirby B, Carr DB, Buchanan ML, Rutherford T, Thummel KE, Fishbein DP, and Unadkat JD (2008) Effects of pregnancy on CYP3A and P-glycoprotein activities as measured by disposition of midazolam and digoxin: a University of Washington specialized center of research study. *Clin Pharmacol Ther* **84**:248–253.

Hogan Q (2002) Distribution of solution in the epidural space: examination by cryomicrotome section. *Reg Anesth Pain Med* **27**:150–156.

Huang W and Isoherranen N (2020) Sampling site has a critical impact on physiologically based pharmacokinetic modelings. *J Pharmacol Exp Ther* **372**:30–45.

Kalvass JC, Olson ER, Cassidy MP, Selley DE, and Pollack GM (2007) Pharmacokinetics and pharmacodynamics of seven opioids in P-glycoprotein-competent mice: assessment of unbound brain EC50,u and correlation of in vitro, preclinical, and clinical data. *J Pharmacol Exp Ther* **323**:346–355.

Ke AB, Greupink R, and Abduljalil K (2018) Drug dosing in pregnant women: challenges and opportunities in using physiologically based pharmacokinetic modeling and dimulations. *CPT Pharmacometrics Syst Pharmacol* **7**:103–110.

Ke AB, Rostami-Hodjegan A, Zhao P, and Unadkat JD (2014) Pharmacometrics in pregnancy: an unmet need. *Annu Rev Pharmacol Toxicol* **54**:53–69.
Kesavan R, Rajan S, and Kumar L (2018) Effect and safety of labor epidural analgesia with intermittent boluses of 0.1% bupivacaine with fentanyl on fetal and maternal outcomes and well-being. *Anesth Essays Res* **12**:769–773.
Kharasch ED, Francis A, London A, Frey K, Kim T, and Blood J (2011) Sensitivity of intravenous and oral alfentanil and pupillary miosis as minimal and noninvasive probes for hepatic and first-pass CYP3A induction. *Clin Pharmacol Ther* **90**:100–108.
Kharasch ED, Russell M, Mautz D, Thummel KE, Kunze KL, Bowdle A, and Cox K (1997) The role of cytochrome P450 3A4 in alfentanil clearance. Implications for interindividual variability in disposition and perioperative drug interactions. *Anesthesiology* **87**:36–50.
Kharasch ED, Walker A, Hoffer C, and Sheffels P (2004) Intravenous and oral alfentanil as in vivo probes for hepatic and first-pass cytochrome P450 3A activity: noninvasive assessment by use of pupillary miosis. *Clin Pharmacol Ther* **76**:452–466.
Labroo RB, Paine MF, Thummel KE, and Kharasch ED (1997) Fentanyl metabolism by human hepatic and intestinal cytochrome P450 3A4: implications for interindividual variability in disposition, efficacy, and drug interactions. *Drug Metab Dispos* **25**:1072–1080.
Loftus JR, Hill H, and Cohen SE (1995) Placental transfer and neonatal effects of epidural sufentanil and fentanyl administered with bupivacaine during labor. *Anesthesiology* **83**:300–308.
Lötsch J (2005) Pharmacokinetic-pharmacodynamic modeling of opioids. *J Pain Symptom Manage* **29**(5, Suppl)S90–S103.
McClain DA and Hug Jr CC (1980) Intravenous fentanyl kinetics. *Clin Pharmacol Ther* **28**:106–114.
Moisés ECD, de Barros Duarte L, de Carvalho Cavalli R, Lanchote VL, Duarte G, and da Cunha SP (2005) Pharmacokinetics and transplacental distribution of fentanyl in epidural anesthesia for normal pregnant women. *Eur J Clin Pharmacol* **61**:517–522.
Morley-Forster PK, Reid DW, and Vandeberghe H (2000) A comparison of patient-controlled analgesia fentanyl and alfentanil for labour analgesia. *Can J Anaesth* **47**:113–119.
Nozari A, Akeju O, Mirzakhani H, Eskandar E, Ma Z, Hossain MA, Wang Q, Greenblatt DJ, and Martyn JAJ (2019) Prolonged therapy with the anticonvulsant carbamazepine leads to increased plasma clearance of fentanyl. *J Pharm Pharmacol* **71**:982–987.
Palm K, Luthman K, Ros J, Gråsjo J, and Artursson P (1999) Effect of molecular charge on intestinal epithelial drug transport: pH-dependent transport of cationic drugs. *J Pharmacol Exp Ther* **291**:435–443.
Palmsten K, Hernández-díaz S, Chambers CD, Mogun H, Lai S, Gilmer TP, and Krista F (2015) The most commonly dispensed prescription medications among pregnant women enrolled in the United States medicaid program. **126**:465–473.
Phimmasone S and Kharasch ED (2001) A pilot evaluation of alfentanil-induced miosis as a noninvasive probe for hepatic cytochrome P450 3A4 (CYP3A4) activity in humans. *Clin Pharmacol Ther* **70**:505–517.
Poole JH (2003) Analgesia and anesthesia during labor and birth: implications for mother and fetus. *J Obstet Gynecol Neonatal Nurs* **32**:780–793.
Rauck R, Oh DA, Parikh N, Koch C, Singla N, Yu J, Nalamachu S, and Vetticaden S (2017) Pharmacokinetics and safety of fentanyl sublingual spray and fentanyl citrate intravenous: a single ascending dose study in opioid-naïve healthy volunteers. *Curr Med Res Opin* **33**:1915–1920.
Reina MA, Franco CD, López A, Dé Andrés JA, and van Zundert A (2009) Clinical implications of epidural fat in the spinal canal. A scanning electron microscopic study. *Acta Anaesthesiol Belg* **60**:7–17.
Reynolds F, Sharma SK, and Seed PT (2002) Analgesia in labour and fetal acid-base balance: a meta-analysis comparing epidural with systemic opioid analgesia. *BJOG* **109**:1344–1353.
Richardson J and Groen GJ (2005) Applied epidural anatomy. *Contin Educ Anaesth Crit Care Pain* **5**:98–100.
Rodgers T and Rowland M (2007) Mechanistic approaches to volume of distribution predictions: understanding the processes. *Pharm Res* **24**:918–933.
Schauberger CW, Newbury EJ, Colburn JM, and Al-Hamadani M (2014) Prevalence of illicit drug use in pregnant women in a Wisconsin private practice setting. *Am J Obstet Gynecol* **211**:255.e1–255.e4.
Shum S and Isoherranen N (2021) Human fetal liver metabolism of oxycodone is mediated by CYP3A7. *AAPS J* **23**:24.
Stanley TH (1992) The history and development of the fentanyl series. *J Pain Symptom Manage* **7**(3, Suppl)S3–S7.
Stanski DR and Hug Jr CC (1982) Alfentanil–a kinetically predictable narcotic analgesic. *Anesthesiology* **57**:435–438.
Topletz AR, Zhong G, and Isoherranen N (2019) Scaling in vitro activity of CYP3A7 suggests human fetal livers do not clear retinoic acid entering from maternal circulation. *Sci Rep* **9**:4620.
Ummenhofer WC, Arends RH, Shen DD, and Bernards CM (2000) Comparative spinal distribution and clearance kinetics of intrathecally administered morphine, fentanyl, alfentanil, and sufentanil. *Anesthesiology* **92**:739–753.
Van de Velde M (2005) Neuraxial analgesia and fetal bradycardia. *Curr Opin Anaesthesiol* **18**:253–256.
Walker MA, Younan Y, de la Houssaye C, Reimer N, Robertson DD, Umpierrez M, Sharma GB, and Gonzalez FM (2019) Volumetric evaluation of lumbar epidural fat distribution in epidural lipomatosis and back pain in patients who are obese: introducing a novel technique (fat finder algorithm). *BMJ Open Diabetes Res Care* **7**:e000599.
Williams JA, Ring BJ, Cantrell VE, Jones DR, Eckstein J, Ruterbories K, Hamman MA, Hall SD, and Wrighton SA (2002) Comparative metabolic capabilities of CYP3A4, CYP3A5, and CYP3A7. *Drug Metab Dispos* **30**:883–891.
Yu C, Yuan M, Yang H, Zhuang X, and Li H (2018) P-glycoprotein on blood-brain barrier plays a vital role in fentanyl brain exposure and respiratory toxicity in rats. *Toxicol Sci* **164**:353–362.
Zhang Z, Imperial MZ, Patilea-Vrana GI, Wedagedera J, Gaohua L, and Unadkat JD (2017a) Development of a novel maternal-fetal physiologically based pharmacokinetic model I: Insights into factors that determine fetal drug exposure through simulations and sensitivity analyses. *Drug Metab Dispos* **45**:920–938.
Zhang Z, Imperial MZ, Patilea-Vrana GI, Wedagedera J, Gaohua L, and Unadkat JD (2017b) Development of a novel maternal-fetal physiologically based pharmacokinetic model I: Insights into factors that determine fetal drug exposure through simulations and sensitivity analyses. *Drug Metab Dispos* **45**:920–938.
Zhang Z and Unadkat JD (2017) Verification of a maternal-fetal physiologically based pharmacokinetic model for passive placental permeability drugs. *Drug Metab Dispos* **45**:939–946.
Ziesenitz VC, König SK, Mahlke NS, Skopp G, Haefeli WE, and Mikus G (2015) Pharmacokinetic interaction of intravenous fentanyl with ketoconazole. *J Clin Pharmacol* **55**:708–717.

Address correspondence to: Nina Isoherranen, University of Washington Health Science Building Room H-272M, Box 357610, Seattle, WA 98195-7610. E-mail: ni2@uw.edu